JOURNAL OF MATERIALS SCIENCE 21 (1986) 103-109

The strength of brass/Sn–Pb–Sb solder joints containing 0 to 10% Sb

W. J. TOMLINSON, N. J. BRYAN
Department of Materials, Coventry Polytechnic, Coventry CV1 5FB, UK

The strength of brass/Sn–Pb–Sb solder joints has been determined for solders containing 0 to 10% Sb and the fracture process examined by microscopical techniques. Intermetallic formation by interdiffusion in the Cu–Zn/Sn–Pb–Sb and Cu–Zn/Pb–Sb systems were also investigated. As the amount of antimony in the solder increases the thickness and hardness of the intermetallic layer increases, and at and above 4% Sb cuboids of SnSb form in the solder. Antimony causes solid-solution strengthening of the joint up to 3% Sb and a ductile fracture occurs at the solder/intermetallic interface. At and above 4% Sb there is a fall in strength with a cleavage type of fracture associated with SnSb in the solder, and at the 8 and 10% Sb levels with fracture in the intermetallic layer. Additions of up to 10% Sb in the solder reduce the shear strength by only 10%, but cause the joint to have a variable and occasionally very low fatigue resistance. Interdiffusion studies show that the Cu–Sn intermetallic phase formed with the antimony-containing solder is not based on the ε-phase, and is probably based on the η-phase in the Cu–Sn–Sb system.

1. Introduction

Tin is the base metal of many solders. It alloys readily at a conveniently low temperature with many common substrates like iron and copper, and also retains its excellent wetting properties when alloyed with lead, antimony, zinc and silver. The Sn–Pb alloys are an important solder series and a number of additions may be made to the solder to improve the joint properties or to replace the tin with a cheaper substitute [1, 2]. Antimony is frequently added to Sn–Pb solders for these reasons. The antimonial tin–lead solders and their properties have been surveyed by Manko [2] and only those aspects important in the present work are outlined. Solid-solution strengthening of tin occurs with up to 7% Sb,* and since the solubility of tin in lead at room temperature is small the solid solution strengthening of Sn–Pb solder by antimony is due mainly to strengthening of the tin. In a 60–40 Sn–Pb alloy, up to about 4.0% Sb may dissolve in the alloy and above 4.0% Sb a primary compound SbSn occurs as cuboids. Antimony up to about 0.5% produces a fall in the contact angle on copper but above 0.5% the effect is relatively small [2, 3]. The strength of raw 60–40 Sn–Pb solder is increased by the addition of antimony [4], and the strength of large joints is increased slightly by addition of antimony up to 1.8% Sb and thereafter it decreases [5]. The creep strength of large joints is also slightly increased by small additions of antimony [5]. Recent studies of a brass/60% Sn–57.8% Pb–2.2% Sb joint has confirmed the strengthening effect of antimony, and has also shown that the presence of antimony results in a greater scatter in the strength properties [6]. More detailed work on a brass/2% Sb solder ring-and-plug joint have shown that the variable strength is probably due to the presence of microporosity at the solder–brass interface and, somewhat surprisingly, the degree of scatter in the fatigue results was much less than in the strength and creep properties [7].

The soldered joint is essentially an interdiffused and then quickly cooled casting, and the properties of the joint depend upon a large number of factors; these include the composition of the solder, substrate, and flux, the reaction time and temperature and hence the amount of interdiffusion of the metals, the cooling rate, internal stress, joint thickness and geometry, and the method of testing. The general effect of the intermetallic layer is to decrease the strength of the joint considerably, e.g. with a Cu/Sn–Pb joint the strength was decreased by over 50% as the layer thickness increased from 4 to 14 μm [8]. The nature and properties of the intermetallic layers are not known in detail and information on interdiffusion in the Cu–Zn/Sn–Pb–Sb system is scarce and inconclusive. Recent work [9] on the interdiffusion of brass and a 58% Sn–40% Pb–2% Sb solder with a 1% Cu + 1% Zn addition showed the formation of a Cu–Sn intermetallic phase containing about equal amounts of copper and tin, but the presence of the compound ZnSb was not detected. It had long been thought that antimonial Sn–Pb solder joints were brittle, and that the brittleness was caused by a ZnSb phase, but examination of failed joints suggested that brittleness was caused by the formation of shrinkage voids which diverted the fracture path away from the intermetallic/solder interface and through the solder itself [9]. Analysis of the Cu–Sn, Cu–Pb, Pb–Zn, and Cu–Sn–Sb phase equilibria [10] indicates that the possible compounds that may form in these systems at soldering temperatures are the $\varepsilon(Cu_3(Sn, Sb))$, β(SnSb), $\eta(Cu_6Sn_5)$,

*All compositions are in wt % unless given otherwise.

0022–2461/86 $03.00 + .12

TABLE I The effect of flux type on the strength of brass/Sn–Pb solder joints*

	Rosin flux		Inorganic flux	
	Shear strength (MPa)	Work to fracture (Nm)	Shear strength (MPa)	Work to fracture (Nm)
Mean	14.7	7.17	20.87	11.42
Standard Deviation	3.179	1.66	1.32	1.22
95% Confidence limit	± 2.27	± 1.19	± 0.94	± 0.87

*Sample size = 10.

and κ phases. The κ phase extends from 0 to 100% Sb and is thought to be the δ-phase of the Cu–Sn and Cu–Sb systems [11].

In view of the complexity of the Cu–Zn/Sn–Pb–Sb solder system the present work aims to establish a reproducible joint manufacturing and testing procedure, and to examine the effect of up to 10% Sb on the microstructure and properties of the soldered joint.

2. Experimental details

A 1 kg master alloy of Sn–40% Pb was air-melted in a "salamander" crucible from tin and lead stock nominally 99.9% pure, and was cast into a mild steel mould and then fettled to remove porosity, dross etc. Separate melts made from the master alloy and containing 1, 2, 3, 4, 6, 8 and 10% Sb were cast as ingots of about 0.3 kg and fettled. The weighed component compositions were taken as the solder nomial composition. The ingots were rolled to 0.25 mm thick and cut to 10 mm × 10 mm pieces as required. The inorganic flux was prepared from Analar materials to specification DTD 87 1953 (250 g $ZnCl_2$, 250 g NH_4Cl, 10 ml HCl, 250 ml distilled water). A proprietary brand of a mildly activated type of rosin flux in a grease base was also used in a limited number of preliminary experiments. The brass substrates were cut from a sheet of 70/30 brass 2.0 mm thick by a bandsaw and were then milled into pieces 15 mm × 80 mm.

To ensure reproducibility in the manufacture of the soldered joints, a jig was made to hold with spring clips two pieces of brass with a fixed gap of 0.10 mm and a fixed (adjustable) overlap. The jig was bolted on to a trolley which ran on rails and protruded so that the whole jig and specimen could be moved easily in and out of a pre-stabilized furnace. Brass specimens in the solder region were prepared dry to a 600 grit finish, degreased in acetone and then fluxed. When the furnace with the empty jig had maintained 450° C for about 2 h it was withdrawn, loaded with the brass specimens containing a 10 mm × 10 mm square of solder in a 14 mm overlap, again fluxed around the edges and then repositioned in the furnace. A thermocouple tip rested on the "step" of the joint, and when this reached 300° C a cold air blast from a hair-drier clamped at one end of the tube furnace was switched on and its position adjusted so that the specimen stayed at 300° C. After 5 min the jig was removed and the joint was air-cooled. The cooling time to about 100° C was approximately 8 min, when the specimen was removed and the process repeated. This process was to overcome the long time-constants and thermal hysteresis in the system, and gave results sufficiently reproducible for the present purpose. When an inorganic flux was used the cold specimens were thoroughly washed in water to prevent post-soldering corrosion.

The specimens were tested in tension in a JJ tensometer with a 20 kN load cell at a load setting of 0.4, a cross-head speed of 5 mm min^{-1} and a cross-head/paper ratio of 5:1. Flat-jawed chucks gripped each end of the specimen to within 5 mm of the joint. The load–extension curves were recorded electronically. The work to fracture was determined using the "paper-cutting and weighing" technique. Limited fatigue data, mainly of a comparative nature, were also obtained on the same machine. So that fracture would occur in a reasonable time, the upper limit was set at 2.7 kN ($\approx$ 0.8 yield stress) and the lower limit 2.0 kN and a fast strain rate of 50 mm min^{-1} used. Limited creep data were also obtained. Creep specimens were fabricated as before but with only a 7 mm overlap, and the width was reduced to 3 mm by milling each side of the specimen with a circular cutting tool leaving radii of about 6 mm from the edge of the overlap region. These were clamped to 3 mm thick steel plates and suspended from a steel frame by a

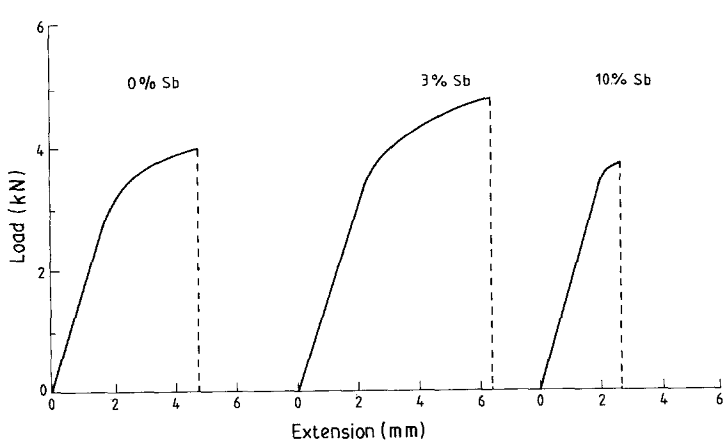

Figure 1 Load–extension curves of brass/Sn–Pb–Sn solder joints containing 0, 3 and 10% Sb.

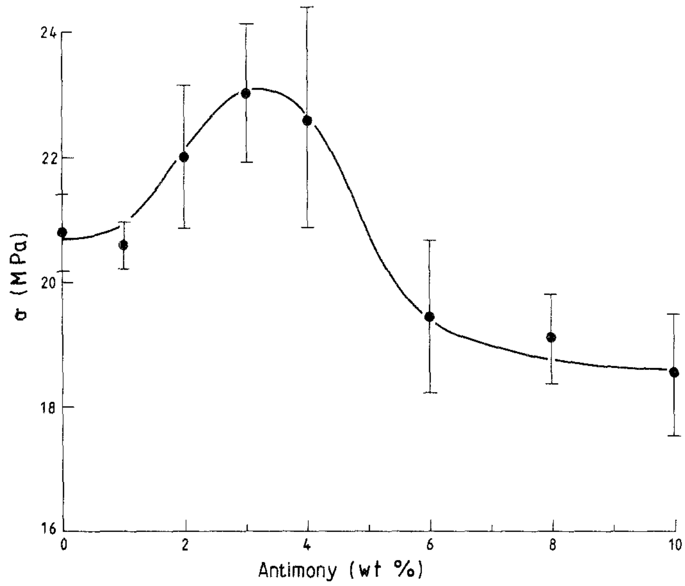

Figure 2 Tensile shear strength σ of brass/Sn–Pb–Sb solder joints.

30 kg load (≈ 0.8 of the tensile yield stress). The specimen was within a furnace held at $80° \pm 2°$ C, and the distance between fiducial marks on the protruding upper and lower steel plates was measured with a travelling microscope.

Various ancillary interdiffusion experiments were performed. Two crucibles were stabilized at 300° C, one contained a $ZnCl_2$–20% NH_4Cl flux with a brass specimen and the other crucible contained the Sn–Pb–Sb alloy with a protective flux covering. After 15 min stabilization in the flux the brass was reacted in the solder for a set time and then air-cooled. The cross-section was then examined metallographically. Some interdiffusion studies were also carried out at 300° C between $\varepsilon(Cu_3Sn)$ and $\eta(Cu_6Sn_5)$ with antimony (from a Pb–10% Sb melt).

Cold-mounting resins were used as part of the standard metallographic techniques. Fracture surfaces and sections were examined using a scanning electron microscope with an attachment for energy-dispersive X-ray analysis.

3. Results and discussion

There is significant scatter in the strengths of soldered joints, and to assess the reproducibility of the present method ten samples fluxed with rosin and ten samples fluxed with $ZnCl_2/NH_4Cl$ were tested in tension. The results are presented in Table I. It is clear that the inorganic flux produces stronger joints with less scatter. Examination of the fracture surfaces showed the inferior wetting characteristics associated with the rosin flux, which produced only a partly-filled joint. In contrast the $ZnCl_2/NH_4Cl$-fluxed joint was full of solder. These observations and results are consistent with recent work [12] in which a $ZnCl_2$ flux was observed to be much more effective than an "organic" flux in decreasing the surface tension of the solder and so promoting wetting of the substrate. From the statistics of Table I we calculate that the sample sizes to detect a change of 2 MPa at the 95% confidence level with the rosin and inorganic fluxes are $n = 20$ and $n = 4$ respectively, and to detect a change of 0.5 MPa the sample sizes are $n = 320$ and $n = 64$ respectively. Working with the inorganic flux it was decided to use a sample size of ten, which enabled a change of 1.2 MPa to be detected at the 95% confidence level.

Typical load–extension curves are shown in Fig. 1 and some derived data in Figs. 2 and 3, for the effect of antimony on the strength of soldered joints. It is seen that the maximum strength occurs with 3% Sb and the fall in strength in the 10% Sb solder compared to the antimony-free solder is 11.1%. The increase in strength is due to the solution-hardening of the tin, and we note that the decrease in strength starting at

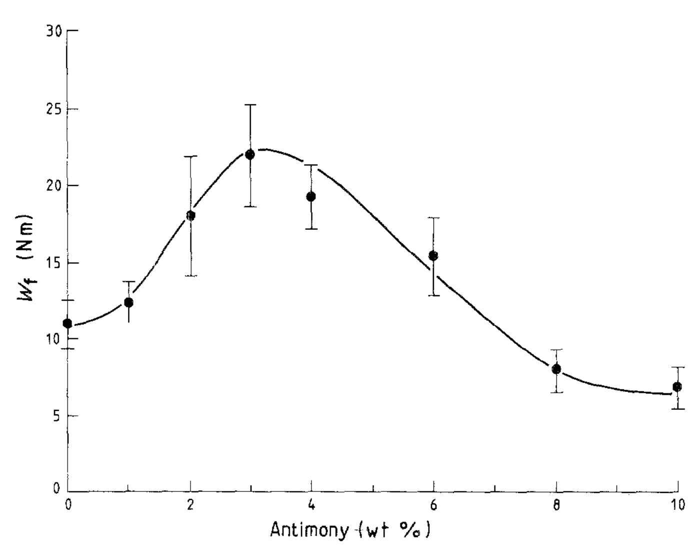

Figure 3 Work to fracture in tension W_f of brass/Sn–Pb–Sb solder joints.

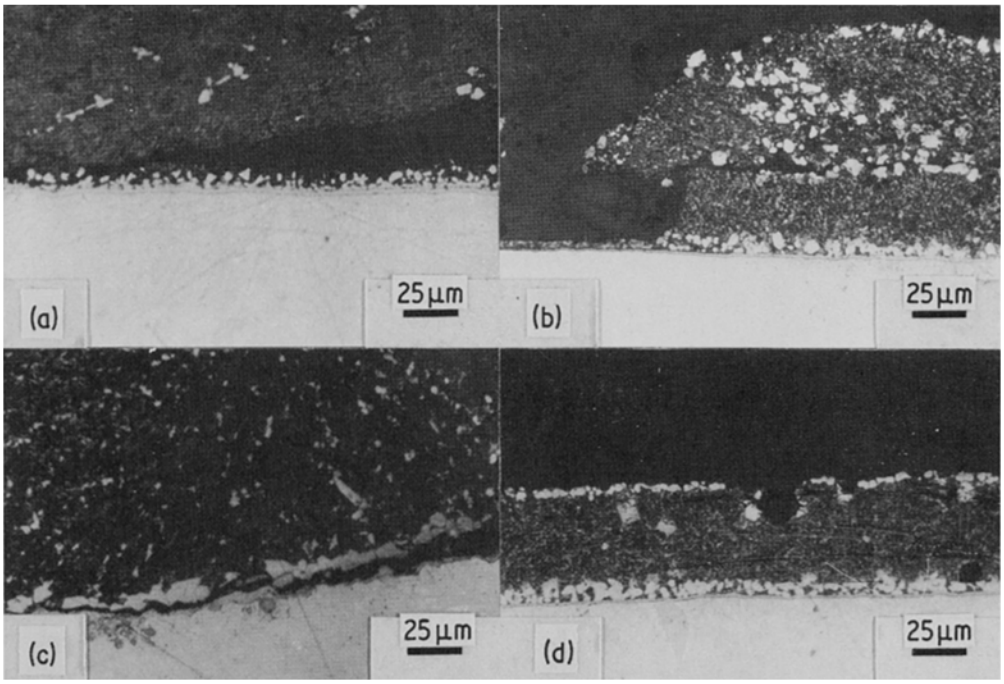

Figure 4 Fracture in tensile tested brass/Sn–Pb–Sb joints. (a) antimony-free solder; fracture path at the solder/intermetallic interface, (b) 6% Sb solder; fracture edge in the intermetallic/solder region, (c) 8% Sb solder; fracture path in the intermetallic layer, (d) 8% Sb solder; fracture edge. Etched in alcoholic ferric chloride with 2% nitric acid.

4% Sb corresponds to the value at which SnSb exists in the Sn–Pb–Sb system [10]. The peak in strength follows the trend of previous work [5], which however showed the peak at 1.8% Sb in contrast to the present value of 3% Sb. However, the solubility of antimony in the Pb–Sn solder varies significantly with temperature [10], and the difference in the composition of the solder at which the peak occurs may be due to differing thermal conditions in the joint affecting the precipitation of SnSb.

Microscopical examination of the solder/brass interface showed a layer of intermetallic phases. The growth and nature of these layers will be discussed in detail later. The fracture path in relation to the intermetallic layer and the presence or absence of precipitated primary SnSb cuboids in the solder is shown in Fig. 4. Joints formed with antimony-free solder generally fractured at the solder/intermetallic layer interface (Fig. 4a). Occasionally the fracture path had been diverted into the solder by isolated porosity. Samples containing 1, 2 and 3% Sb had fractured both at the solder/layer interface and through the intermetallic layer, with the fracture path often alternating

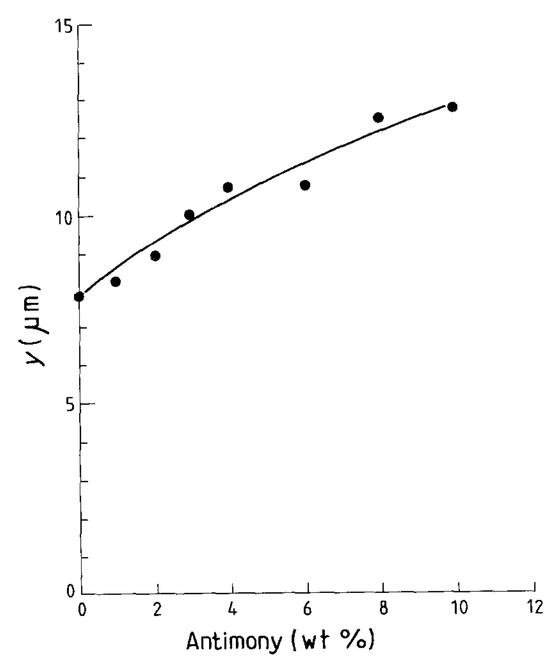

Figure 5 Intermetallic thickness y formed in the Cn–Zn/Sn–Pb–Sb system at 300° C for 5 min.

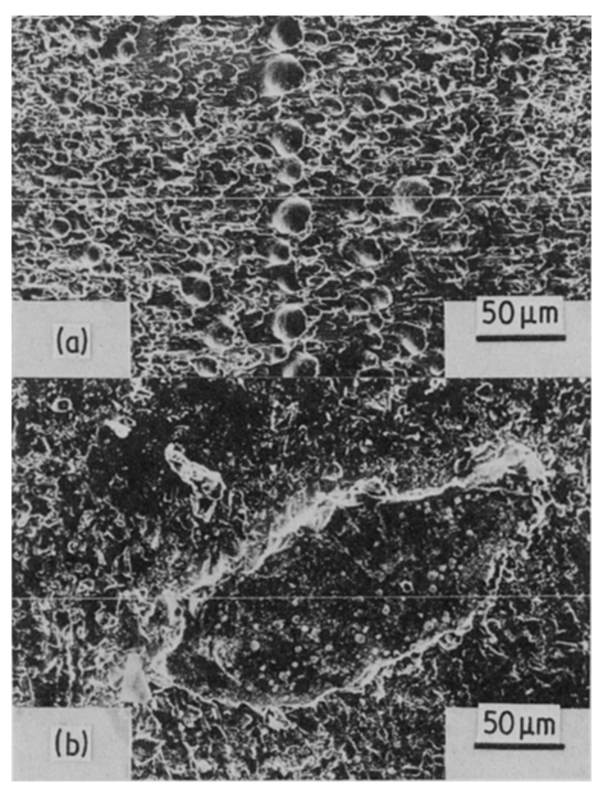

Figure 6 Fracture surfaces of tensile tested brass/Sn–Pb–Sb joints. (a) Antimony-free solder; ductile fracture, (b) 10% Sb solder; cleavage-like fracture.

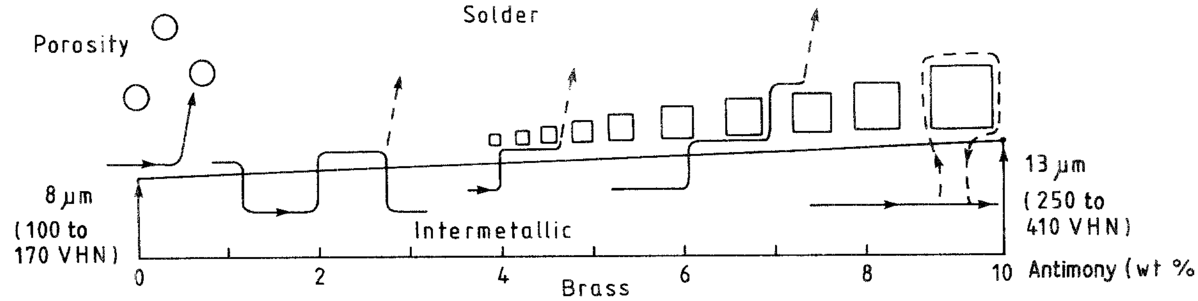

Figure 7 Schematic microstructure and fracture behaviour in brass/Sn–Pb–Sb solder joints. Fracture path —→—. Fracture path (occasional) - - → - -.

between the two. Primary precipitates of SnSb were observed in all solders at and above 4% Sb, and the size of the cuboids was larger as the amount of antimony in the solder increased. Samples containing 4 and 6% Sb had either fractured through the intermetallic layer or via SnSb precipitates in the solder (Fig. 4b), while in the sample containing 8 and 10% Sb the fracture path was mainly within the intermetallic layer and not at either interface (Fig. 4c and d). We note in Fig. 4d how a large cuboid of SnSb (now missing) has temporarily changed the fracture path. As the amount of antimony in the solder increased both the thickness (Fig. 5) and the hardness of the intermetallic layer increased. The hardness of the layer in the solders containing 0 and 10% Sb was 100 to 170 and 250 to 410 Vickers Hardness Number respectively.

Semi-quantitative data on the composition of the intermetallic layer are presented in Table II. It is seen that a substantial amount of zinc is present throughout the layer and the antimony substitutes for roughly equal amounts of tin and copper. Examination of the fracture surfaces on the antimony-free joint showed the compositions to be Sn : Pb about 60 : 40 on one face and Cu : Sn about 50 : 50 on the other face, thus confirming the fracture to be at the solder/intermetallic interface (see also Fig. 4a). The fracture was ductile (Fig. 6a). The fracture in the 10% Sb joint showed a mixed brittle and ductile fracture (Fig. 6b). The region surrounding the central area showed a fracture with cleavage characteristics and contained Cu : Sn : Sb approximately 45 : 45 : 10. The central "void" region appeared to fracture in a more ductile manner and contain much less antimony.

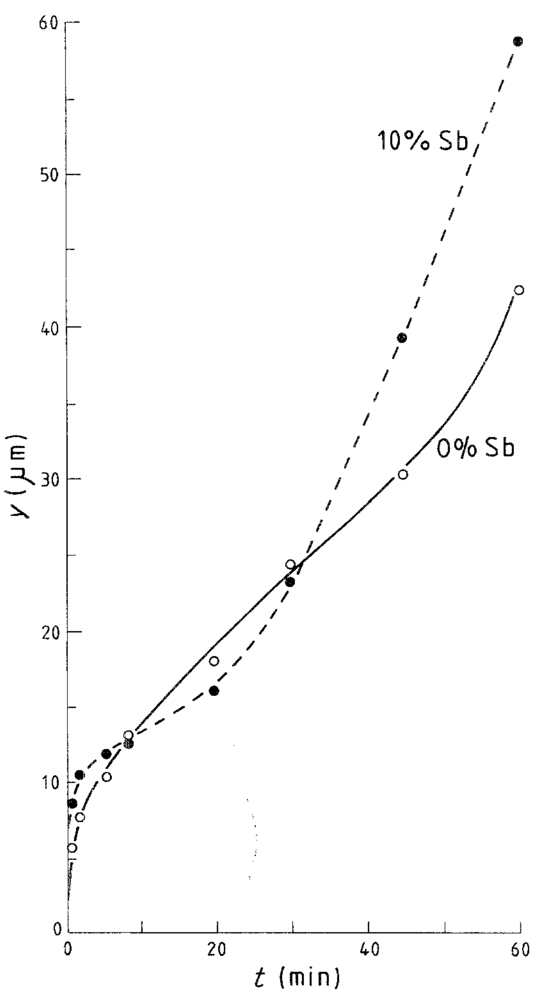

Figure 8 Intermetallic thickness y formed in the Cu–Zn/Sn–Pb–Sb system at 300° C for various times t.

The present data show a clear pattern of the effect of antimony on the strength of brass/Sn–Pb solder joints. The fracture processes are summarized in Fig. 7. When the solder contains no antimony, the joint fractures in a ductile manner at the solder/intermetallic interface. The path is frequently diverted to gas microvoids in the solder as observed by other workers [7, 9] but the effect is not considered crucial in the present case. The increase in strength up to 3% Sb (Fig. 2) is due to solid-solution hardening of tin in the solder by antimony. As the amount of antimony in the solder increases, the thickness (Fig. 5) and hardness of the intermetallic layer increases and there is an increased tendency for the fracture to occur in the layer. At and above 4% Sb, cuboids of SnSb occur in the solder because the solubility of antimony in the 60% Sn–40% Pb solder has been exceeded and there is a decrease in strength (Fig. 2). Non-uniform dispersions of SnSb as clusters or stringers frequently provide easy alternative fracture paths along the solder/SnSb interfaces. However, at sufficiently high antimony contents it appears that the increased thickness and hardness of the intermetallic layer favours fracture within the intermetallic layer.

Some aspects of the nature of the intermetallic layer were investigated in an associated interdiffusion study. Growth curves for the formation of the layers in solders containing 0 and 10% Sb with brass are shown in Fig. 8, and it is seen that no regular pattern occurs. It has been stated that the intermetallic phase is Cu_6Sn_5 [7]. The data of Table II are only semi-quantitative and do not allow identification of the intermetallic phase. However, a limited separate study on the interdiffusion of antimony (from a Pb–10% Sb solution) at 300° C for up to 1 h showed that negligible

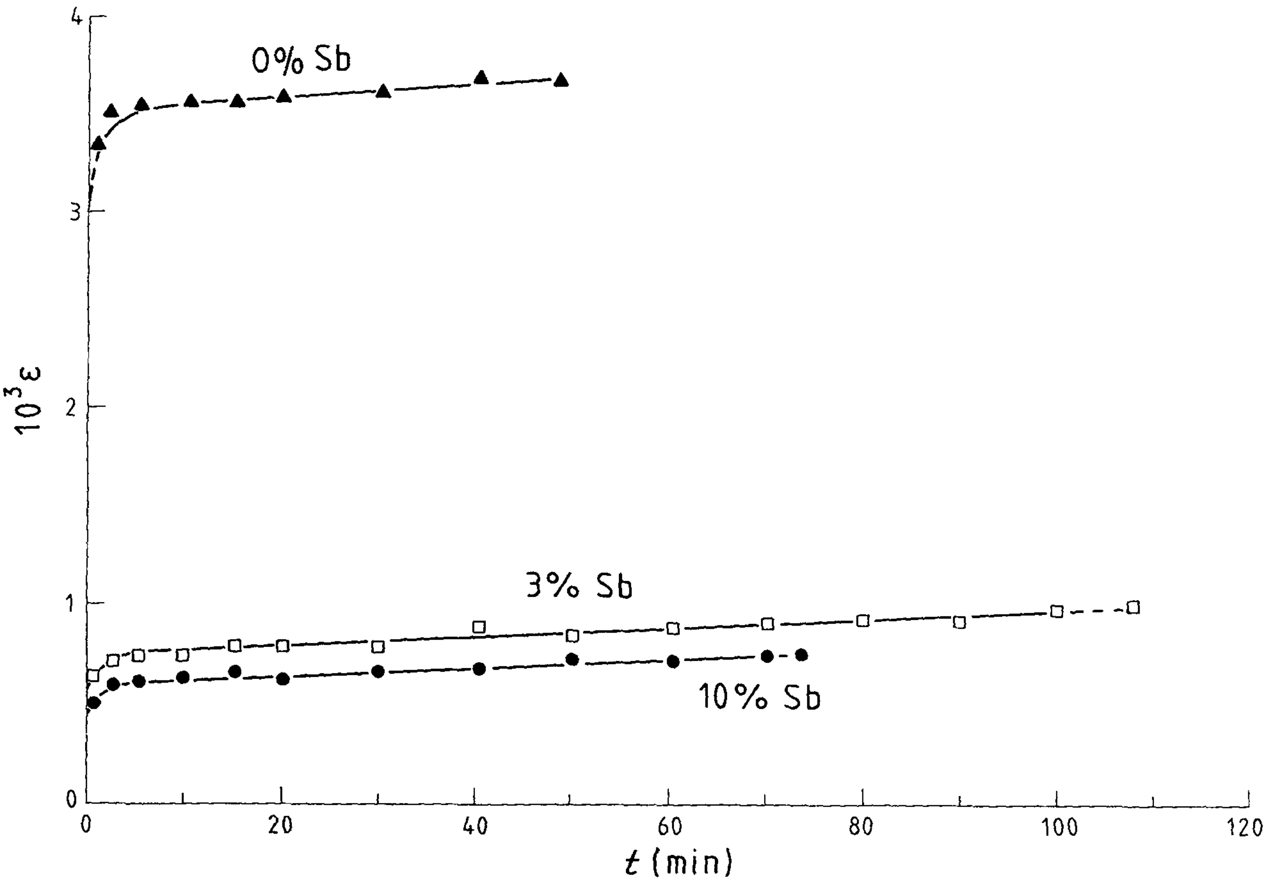

Figure 9 Creep curves (strain ε against time t) for brass/Sn–Pb–Sb solder joints tested at 80° C. Load 30 kg.

diffusion of antimony in the ε phase occurs but rapid and substantial penetration occurred in the η phase. The interface in the η phase was difficult to define, but the approximate penetration depths after 1, 2, 5, 10, 20, 30 and 60 min were 85, 130, 290, 490, 1300, 1850 and 2000 μm respectively. On the basis of the high solubility of antimony in Cu_6Sn_5 we conclude that the intermetallic layer is probably based on the Cu_6Sn_5 phase.

The present work shows that antimonial solder containing up to 10% Sb does not cause any significant brittleness as indicated by the strength and work to fracture properties. Limited creep data (Fig. 9) also do not indicate any pronounced tendency to brittleness. However, some fatigue data (Table III) show that the antimonial solder joint has a lower resistance to fatigue, and in some cases the resistance may be exceptionally low. No associated microscopical studies have been made, but it is probable that the large variation in fatigue resistance is due to the large variation in SnSb clustering observed in the tensile fracture studies. And it may be that the poor reputation antimonial solder joints have with respect to brittleness is due to their variable and often very low fatigue resistance.

TABLE II Approximate composition (wt %) of the intermetallic layer formed on brass during soldering

Element	Near bass		Near solder	
	0% Sb	10% Sb	0% Sb	10% Sb
Sn	43	34	43	36
Pb	2	2	2	2
Sb	0	18	0	21
Cu	44	37	44	33
Zn	11	9	11	8

Acknowledgement
The authors wish to thank Dr R. Carey for help with the scanning electron microscopy.

References

1. B. T. K. BARRY and C. J. THWAITES, "Tin and its Alloys and Compounds" (Pergamon, London, 1984) p. 88.
2. H. H. MANKO, "Solders and Soldering," 2nd Edn. (McGraw Hill, New York, 1979) p. 101.
3. M. L. ACKROYD, C. A. MACKAY and C. J. THWAITES, *Metals Tech.* (February 1975) 73.
4. W. A. BAKER, *J. Inst. Metals.* **65** (1939) 277.
5. S. J. NIGHTINGALE and O. F. HUDSON, "Research Monograph No. 1" (British Non-Ferrous Metals Research Association, London, 1942).

TABLE III Fatigue testing of brass/Sn–Pb–Sb solder joints*

Sample No.	Cycles to failure	
	0% Sb	10% Sb
1	3459	64
2	2040	5166
3	2303	137
4	4595	1565
5	3603	4096
6	2103	4173
7	1967	636
8	3705	533
9	4031	1835
10	1985	3742
Mean	2979	2195
Standard deviation	948	1823

*Maximum load 2.75 kN, minimum load 2.0 kN, strain rate 50 mm min^{-1}.

6. K. R. STONE, R. DUCKETT, S. MUCKETT and M. WARWICK, *Brazing and Soldering* No. 4 (1983) 20.
7. C. J. THWAITES and D. McDOWALL, *ibid* No. 6 (1984) 32.
8. R. A. HAGSTROM and R. N. WILD, in Proceedings of International National Electronic Packaging Conference, Brighton, October 1969 (Kiver Publications Inc) p. 271.
9. Report of the International Tin Research Council (Spring 1982) p. 14.
10. "Metals Handbook", Vol. 5 (American Society for Metals, 1979).
11. M. TASAKI, *Mem. Coll. Sci. Kyoto Imp. Univ.* **12** (1929) 227.
12. F. H. HOWIE and E. D. HONDROS, *J. Mater. Sci.* **17** (1982) 1434.

Received 24 July
and accepted 18 December 1984